nature geoscience

LETTERS

PUBLISHED ONLINE: 9 MARCH 2015 | DOI: 10.1038/NGEO2382

Photosynthetic seasonality of global tropical forests constrained by hydroclimate

Kaiyu Guan[1,2*], Ming Pan[1], Haibin Li[3], Adam Wolf[4], Jin Wu[5], David Medvigy[6], Kelly K. Caylor[1], Justin Sheffield[1], Eric F. Wood[1], Yadvinder Malhi[7], Miaoling Liang[1], John S. Kimball[8,9], Scott R. Saleska[5], Joe Berry[10], Joanna Joiner[11] and Alexei I. Lyapustin[11]

The response of tropical forests to droughts is highly uncertain[1]. During the dry season, canopy photosynthesis of some tropical forests can decline, whereas in others it can be maintained at the same or a higher level than during the wet season[2]. However, it remains uncertain to what extent water availability is responsible for productivity declines of tropical forests during the dry season[2,3]. Here we use global satellite observations of two independent measures of vegetation photosynthetic properties (enhanced vegetation index from 2002 to 2012 and solar-induced chlorophyll fluorescence from 2007 to 2012) to investigate links between hydroclimate and tropical forest productivity. We find that above an annual rainfall threshold of approximately 2,000 mm yr^{-1}, the evergreen state is sustained during the dry season in tropical rainforests worldwide, whereas below that threshold, this is not the case. Through a water-budget analysis of precipitation, potential evapotranspiration and satellite measurements of water storage change, we demonstrate that this threshold determines whether the supply of seasonally redistributed subsurface water storage from the wet season can satisfy plant water demands in the subsequent dry season. We conclude that water availability exerts a first-order control on vegetation seasonality in tropical forests globally. Our framework can also help identify where tropical forests may be vulnerable or resilient to future hydroclimatic changes.

Photosynthetic metabolism in tropical forests controls ecosystem carbon uptake from the atmosphere, and it also influences critical ecosystem services, including carbon storage[4], freshwater delivery[5], maintenance of biodiversity[5], and regulation of regional and global climate[6]. The photosynthetic metabolism of many tropical forests exhibits a recurring seasonality[2,7]. Understanding how climate influences these seasonal dynamics is an essential prerequisite for realistically predicting tropical forest responses to inter-annual and longer-term climate variation and change[3]. In particular, with a wide spectrum of varying total annual precipitation and dry-season length in the tropics (Supplementary Fig. 7), the extent to which seasonality of vegetation productivity in tropical forests responds to water limitation remains unclear[2,3]. Although tropical forest seasonal dynamics have been studied at site and regional scales using eddy flux-tower networks and/or satellite remote sensing in Amazonia[2,8,9], Insular Southeast (SE) Asia[7] and Africa[10], a globally consistent functional inter-comparison of tropical forests is lacking. Thus, in this paper we address the following questions: What is the extent to which the seasonality of vegetation photosynthesis is limited by water availability in global tropical forests? Are there critical environmental thresholds that explain these seasonal variations? If so, what are the underlying physical mechanisms? What are the implications of such mechanisms on the future of tropical forests under climate change?

We address the above questions by analysing the wet- and dry-season difference in two independent and remotely sensed measures of vegetation photosynthetic properties: the enhanced vegetation index (EVI; ref. 11), a proxy for vegetation greenness and photosynthetic potential[7] from the MODerate resolution Imaging Spectroradiometer (MODIS) collection 5 for the period 2002–2012; solar-induced chlorophyll fluorescence (SIF), which is sensitive to the electron transport rate of plant photosynthesis as well as the fraction of absorbed radiation[12,13], from the Global Ozone Monitoring Experiment-2 (GOME-2) for the period 2007–2012 (Supplementary Information). Both satellite-derived photosynthetic metrics also implicitly include information on forest canopy structure. Possible artefact of sun-sensor geometry in the MODIS EVI data has been addressed in Supplementary Information. The seasonal patterns of these two photosynthetic metrics are validated against gross primary production (GPP) ground estimates from eight flux towers in the Amazon (Supplementary Information). We define 'dry season' as the period when monthly accumulated precipitation (P) is less than the potential plant water need estimated from potential evapotranspiration (PET); conversely, the 'wet season' is defined for months when $P \geq PET$. Both P and PET are derived primarily from satellite observations (for example, from the Tropical Rainfall Measuring Mission, TRMM, see Methods and Supplementary Information). In our analysis, we extract wet- and dry-season EVI separately for each year, calculate their differences, and normalize the results by their annual mean values (denoted as $\Delta EVI_{(wet-dry)}$) for each grid cell. We apply the same calculation for SIF ($\Delta SIF_{(wet-dry)}$). Thus, positive $\Delta EVI_{(wet-dry)}$ (or $\Delta SIF_{(wet-dry)}$) means

[1]Department of Civil and Environmental Engineering, Princeton University, Princeton, New Jersey 08544, USA. [2]Department of Earth System Science, Stanford University, Stanford, California 94305, USA. [3]Department of Earth and Planetary Sciences, Rutgers University, Piscataway, New Jersey 08854, USA. [4]Department of Ecology and Evolutionary Biology, Princeton University, Princeton, New Jersey 08544, USA. [5]Department of Ecology and Evolutionary Biology, University of Arizona, Tucson, Arizona 85721, USA. [6]Department of Geosciences, Princeton University, Princeton, New Jersey 08544, USA. [7]School of Geography and the Environment, University of Oxford, South Parks Road, Oxford OX1 3QY, UK. [8]The University of Montana Flathead Lake Biological Station, Polson, Montana 59860, USA. [9]Numerical Terradynamic Simulation Group, University of Montana, Missoula, Montana 59812, USA. [10]Department of Global Ecology, Carnegie Institution of Washington, 260 Panama Street, Stanford, California 94305, USA. [11]National Aeronautics and Space Administration Goddard Space Flight Center, Greenbelt, Maryland 20771, USA. *e-mail: kaiyug@stanford.edu

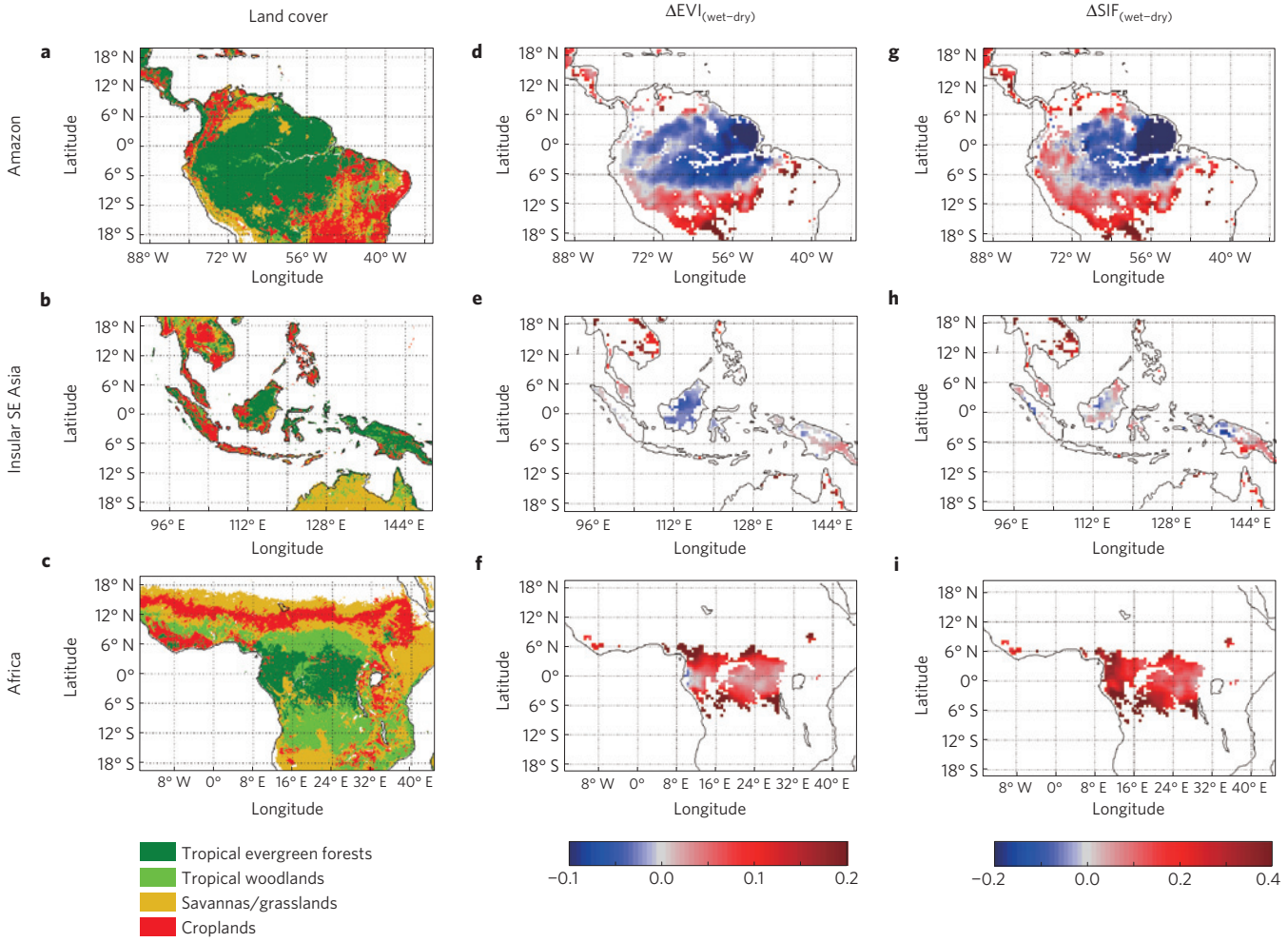

Figure 1 | Multi-year average of normalized wet-/dry-season difference of the photosynthetic properties for the global tropical evergreen forest regions. **a**–**i**, Dominant vegetation types in the tropics of Amazonia, Insular SE Asia, and Africa (**a**–**c**); normalized wet-/dry-season difference for EVI ($\Delta EVI_{(wet-dry)}$) (**d**–**f**) and for SIF ($\Delta SIF_{(wet-dry)}$) (**g**–**i**). The statistical significance of $\Delta EVI_{(wet-dry)}$ and $\Delta SIF_{(wet-dry)}$ patterns are quantified as percentiles of the *t*-test distribution under the null hypothesis that $\Delta EVI_{(wet-dry)}$ (and $\Delta SIF_{(wet-dry)}$) is equal to zero at the grid level, with the results shown in Supplementary Fig. 6.

that the corresponding vegetation property during the wet season is greater than its dry-season condition, indicating sensitivity to seasonal water limitation. In contrast, grids with near-zero or negative $\Delta EVI_{(wet-dry)}$ (or $\Delta SIF_{(wet-dry)}$) indicate that these tropical forests have no apparent response to dry-season water stress. The *t*-test is used to determine statistical significance of the $\Delta EVI_{(wet-dry)}$ and $\Delta SIF_{(wet-dry)}$ pattern (Supplementary Information). We apply our analysis to all tropical evergreen forests between latitudes 20° N and 20° S identified from a global land cover classification (Fig. 1a–c and Supplementary Information).

We find that the global pattern of tropical forest photosynthetic seasonality is a tale of two forests, as shown consistently from both EVI and SIF analyses. Tropical evergreen forests of Africa, southern Amazonia and peripheral Insular SE Asia show predominantly and significantly positive $\Delta EVI_{(wet-dry)}$ and $\Delta SIF_{(wet-dry)}$ (Fig. 1d–i and Supplementary Fig. 6); thus we infer that forest canopy photosynthetic activities are sensitive to water stress in these areas and co-vary with precipitation seasonality. In contrast, $\Delta EVI_{(wet-dry)}$ and $\Delta SIF_{(wet-dry)}$ in central Amazonia and the core of Insular SE Asia are close to zero or significantly negative (Fig. 1d,e,g,h and Supplementary Fig. 6), suggesting that these regions can maintain photosynthetic activity in the dry season at levels similar to or even stronger than in the wet season. Although small discrepancies between $\Delta EVI_{(wet-dry)}$ and $\Delta SIF_{(wet-dry)}$ exist in the wettest part of the tropical forests (that is, west Amazon and central Insular SE Asia) due to combined effects of very few dry-season observations and more pronounced cloudiness effects (especially for SIF), most of these discrepancies are not statistically significant (Supplementary Fig. 6). Collectively, these findings synthesize a diverse suite of previous regional studies that found close correspondence between the seasonality of photosynthetic capacity of tropical evergreen forests and precipitation in southern Amazonia[14] and Africa[10]; and dry-season 'green-up'[2,8,15–17], or at least no 'brown-down'[18], in central Amazonia and Insular SE Asia[7].

The similar spatial clustering pattern between $\Delta EVI_{(wet-dry)}$ (and $\Delta SIF_{(wet-dry)}$) and mean annual precipitation (MAP) (Supplementary Fig. 7) suggests that total precipitation amount may be an indicator of the extent to which tropical forests respond to seasonal water stress. We observe that a simple MAP threshold of approximately 2,000 mm yr^{-1} (Fig. 2a,b; Methods) can effectively distinguish positive and negative regimes of $\Delta EVI_{(wet-dry)}$ and $\Delta SIF_{(wet-dry)}$. Below this threshold, EVI (and SIF) is predominantly lower in the dry season than the wet season (that is, water availability is a limiting factor); above the precipitation threshold, dry-season EVI (and SIF) is either similar to or even significantly higher than its wet-season condition. Thus, distinctive seasonalities in EVI and SIF largely follow regional differences in annual total rainfall within the study region. 90% of African tropical evergreen

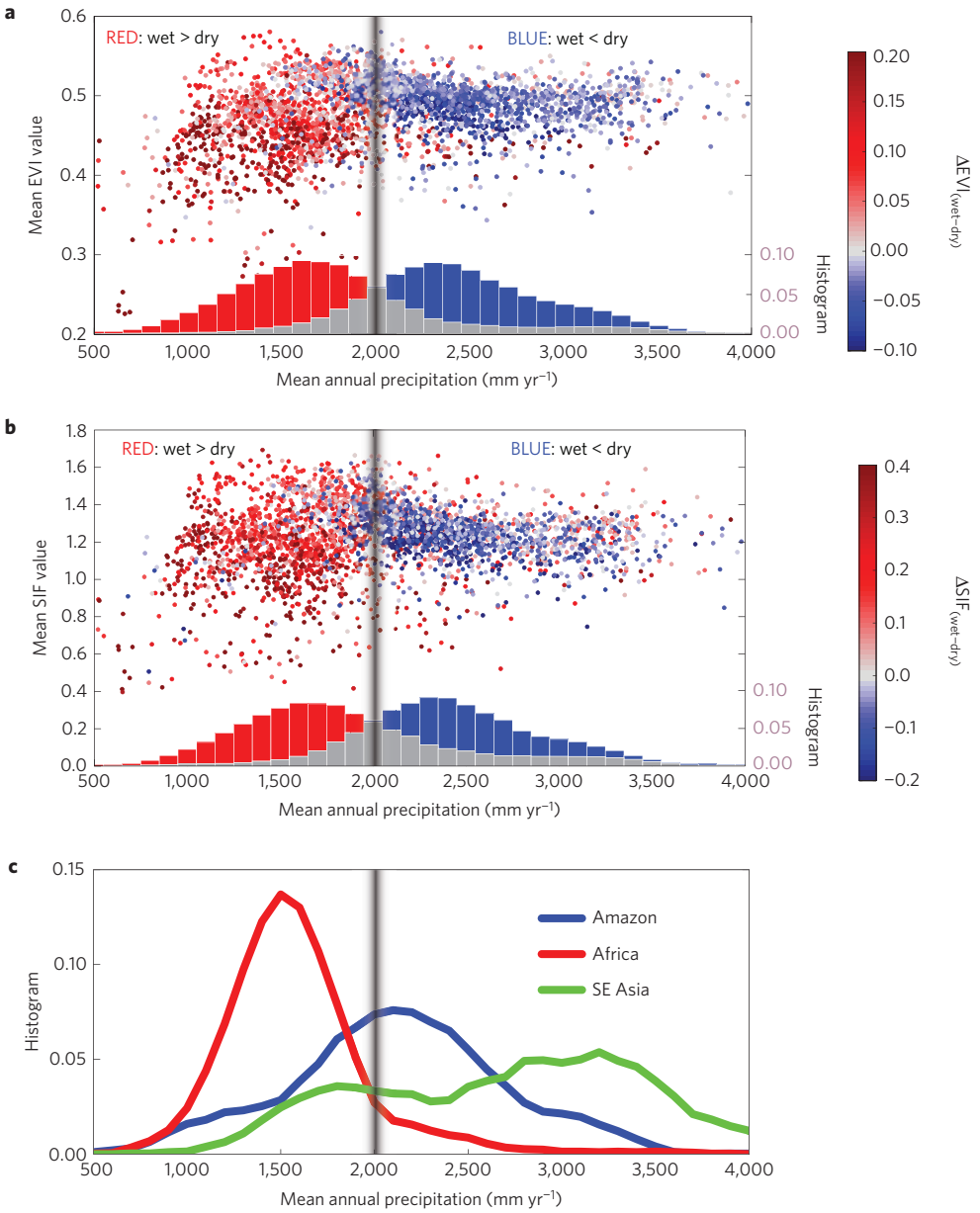

Figure 2 | Associations between total precipitation and wet-/dry-season difference in satellite-inferred photosynthetic properties. a,**b**, Mean annual precipitation versus mean annual EVI and SIF for global tropical evergreen forest grid cells between 20° N and 20° S, colour shaded by the values of $\Delta EVI_{(wet-dry)}$ and $\Delta SIF_{(wet-dry)}$, whose corresponding histograms are shown at the bottom (bin size 100 mm yr^{-1}). **c**, MAP distribution for the three tropical forest regions (year 1998–2012) from TRMM. The vertical grey bar denotes the 2,000 mm yr^{-1} MAP threshold.

forest areas are below the 2,000 mm yr^{-1} threshold; in contrast, 78% of SE Asia forest areas exceed this threshold, whereas Amazonian tropical evergreen forests have 59% above and 41% below the threshold (Fig. 2c and Supplementary Fig. 7). Our finding of a globally applicable MAP threshold corroborates earlier eddy-covariance studies in Amazonia that suggested a similar (~1,900 mm yr^{-1}) rainfall threshold distinguishing whether canopy evapotranspiration covaries with radiation or precipitation[3,9].

What is the basis for a globally applicable precipitation threshold in explaining photosynthetic seasonality in tropical forests? We argue that its physical basis stems from the underlying water supply constraint on canopy photosynthetic metabolism. We hypothesize that precipitation greater than approximately 2,000 mm yr^{-1} is sufficient to sustain plant water needs throughout the year so that water is not a limiting factor for photosynthesis. Rainfall and potential plant water needs (that is, PET) have different seasonal dynamics, resulting in a water surplus during the wet season. Part of this surplus is stored in the subsurface and part is lost through runoff, subsurface flow or deep drainage[19]. During the dry season, there is a water deficit calculated as the cumulative difference between PET and precipitation (Fig. 3a). Dry-season plant water demands can be satisfied to various extents through the use of subsurface water storage—that is, water carried over from the preceding wet season (Fig. 3b). Hence the best way to understand the apparent precipitation threshold is to determine how much rainfall is sufficient to generate enough seasonal carry-over supply for dry-season consumption so that the plant water demand is satisfied all year round.

To assess this dry-season water supply–demand relationship, we analyse regional terrestrial water storage changes derived from the Gravity Recovery and Climate Experiment (GRACE) satellite[20] to quantify the 'release from water storage' during each dry season

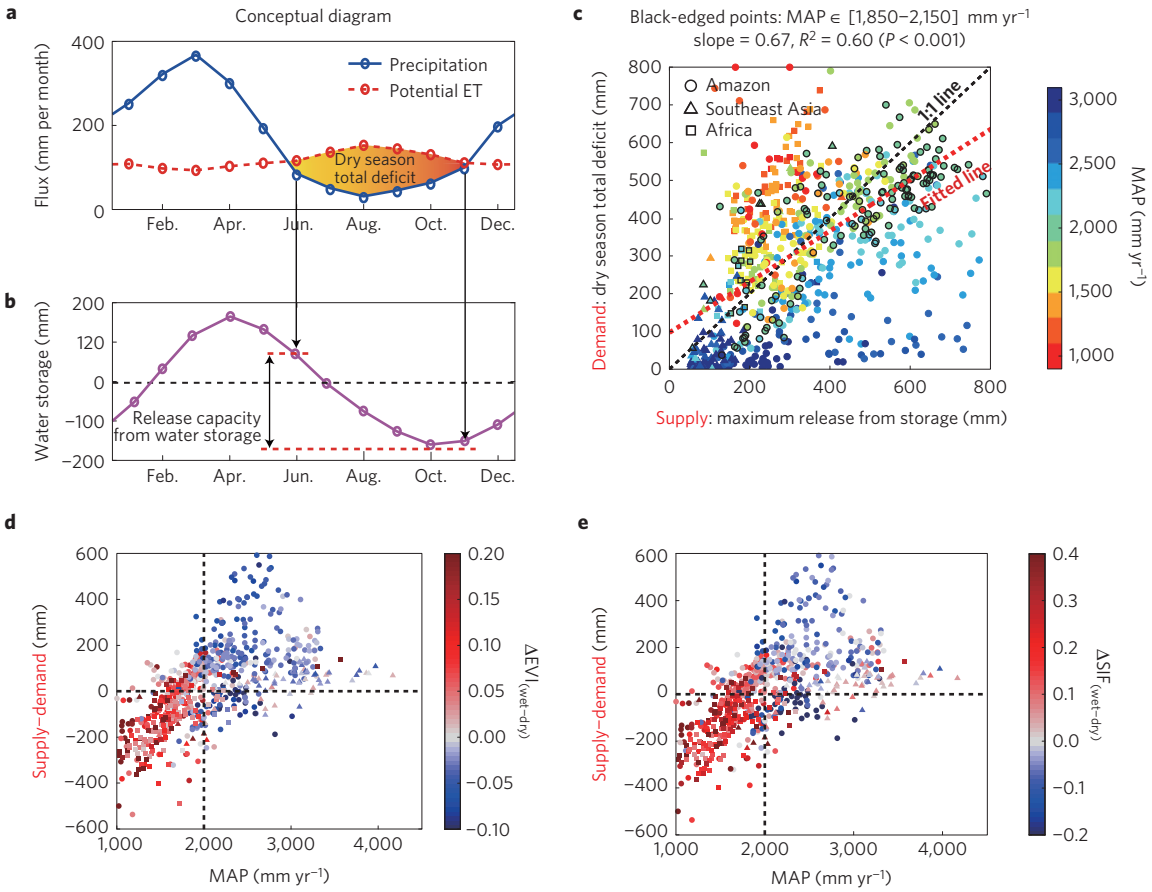

Figure 3 | Relationship between 'dry-season total deficit' and 'maximum release from water storage' in global tropical evergreen forests. a,**b**, Definition of 'dry-season total deficit' (demand) and 'maximum release from water storage' (supply) during the dry season. **c**, Supply–demand relationship, colour shaded with MAP value and shaped for different regions. Black-edged points have MAP between 1,850 and 2,150 mm yr^{-1}, and the linear fitting of these points (red line) has a slope of 0.67 with $R^2 = 0.60$ (p-value < 0.001). **d**,**e**, $\Delta EVI_{(wet-dry)}$ and $\Delta SIF_{(wet-dry)}$ as a function of MAP and (supply–demand) as defined before.

from 2002 to 2012 (see Supplementary Information). For each grid cell, we plot the maximum 'release from water storage' (supply) and averaged 'dry-season total water deficit' (demand) in Fig. 3c. Note that the GRACE-derived dry-season storage release only provides an upper limit on the water supply used by plants, because not all of the released water storage is consumed by plants[19]. The 1:1 line in Fig. 3c critically identifies whether the maximum water supply can satisfy potential demand (below the 1:1 line) or not (above it); the grids cluster above and below the 1:1 line for respective lower and higher annual rainfall levels, indicating that more annual rainfall yields a higher likelihood for seasonal carry-over of water storage to meet dry-season total deficit. We find that grids with MAP ranging from about 1,850–2,150 mm yr^{-1} cluster along the 1:1 line, whereas other rainfall regimes deviate away from this line (Supplementary Fig. 10). Thus the 1,850–2,150 mm yr^{-1} precipitation range defines an apparent transition between two distinct regimes of the dry-season water supply–demand relationship (with wetter grids mostly below the 1:1 line and vice versa). This rainfall range is consistent with the aforementioned 2,000 mm yr^{-1} threshold from Fig. 2. Regional differences in the three tropical evergreen forest regions are also distinguished in Fig. 3c (and Supplementary Fig. 11), consistent with our analysis of hydroclimatic controls on photosynthetic seasonality: African grids are almost all above the 1:1 line; SE Asian grids almost all cluster in a small region below the 1:1 line and within 200 mm of the 'maximum release from water storage'; Amazonian grids are mostly located below the 1:1 line, whereas peripheral areas (for example, southern Amazonia) are directly adjacent to or above the 1:1 line. An independent water-budget quantification at the basin scale[21] (Supplementary Fig. 13) reveals that 39.8% of the total dry-season water supply in the Amazon basin is from the previous wet-season water storage, compared with only 14.4% in the Congo basin, which further corroborates our findings that Amazon and African tropical forests have different seasonal carry-over capacity of subsurface water storage.

These results are summarized by combining MAP and the dry-season water states (that is, supply–demand) together with $\Delta EVI_{(wet-dry)}$ and $\Delta SIF_{(wet-dry)}$ in Fig. 3d,e. Positive values of $\Delta EVI_{(wet-dry)}$ and $\Delta SIF_{(wet-dry)}$ are clustered in the lower-left quadrant, where MAP is below 2,000 mm yr^{-1} and maximum release from storage (supply) is smaller than the dry-season water deficit (demand). Thus, our analysis brings together multiple independent satellite data records (for example, EVI from MODIS, SIF from GOME-2, water storage changes from GRACE, and rainfall from TRMM) into a single coherent framework that reconciles debate about the fundamental limits on the photosynthetic seasonality of global tropical forests. Multiple independent lines of evidence and a converging threshold lend strong credibility to our finding that the water balance constraint is a first-order control on tropical forest photosynthetic seasonality.

Prominence of the water balance as a controlling factor does not preclude the possible importance of other factors such as vegetation type and species diversity. Indeed, ecological and evolutionary mechanisms are likely to converge with hydrologic constraints by structuring the assembly of vegetation communities whose varying

functional traits are matched to each region's hydrologic potential and subsurface water dynamics (including groundwater)[22]. For example, deeply rooted tropical trees (up to 15 m; ref. 23) may have an advantage where access to subsurface water storage is critical for sustaining dry-season plant functioning (for example, eastern Amazonia)[22,23], whereas more deciduous tree communities may occur in regions where wet-season water supply is insufficient to sustain the evergreen habit through the dry season[24]. A global water-table depth product (Supplementary Information) supports this finding by estimating that the characteristic groundwater-table depth in tropical forest regions is roughly 10 ± 3 m where MAP is approximately 2,000 mm yr^{-1}, and is still accessible by the deep-rooted forests in these regions.

In addition to the annual total precipitation as a first-order control on tropical ecosystem functioning, our results also demonstrate the importance of rainfall seasonality, in that longer or more intense dry seasons can lead to a dry-season reduction in photosynthetic properties under a fixed total annual rainfall (Supplementary Fig. 9). Landscape heterogeneities, such as soil properties, nutrients status, topography, and disturbance may play important roles at local to regional scales, and these variabilities may also explain some scatter in our global-scale results. The physiological reasons why EVI and SIF increase during the dry season in many tropical rainforests, corroborated by the flux-tower observation (Supplementary Fig. 5), have not been fully understood, and different theories (for example, leaf phenology[2] and radiation limitation[3,15]) have been proposed and should be further explored. However, a convergent point in all of these theories is that water is not limiting at the seasonal scale in those humid tropical forests.

The identification of a hydroclimate-based mechanism underlying divergent vegetation dynamics of global tropical forests has important implications for forest vulnerability to climate change. Our defined precipitation threshold corresponds to the separation, in the classic Holdridge Life Zone classification system, between moist and dry tropical forests, with dry-season deciduous or semi-deciduous forests composing significant parts of the latter[25]. If there is a species composition ecotone across this MAP threshold, any temporal shift in rainfall regime across this ecotone might be expected to promote associated decline and turnover of large evergreen canopy trees, with concomitant changes in species composition. We also expect regional and continental differences in tropical forest drought sensitivity at the inter-annual level, because the seasonal water carry-over capacity buffer varies geographically (Supplementary Fig. 13). High drought sensitivity found in tropical African rainforests[26] confirms that these areas have low buffering capacity for mitigating drought (see Supplementary Fig. 13). In contrast, most Amazon forests have greater buffering capacity to endure small or short-term droughts. However, our analysis also suggests that many Amazon forests function as a threshold system that would have higher climate risk in severe or extended drought conditions[27,28]. This risk may be further exacerbated by anthropogenic deforestation, land-use changes and fire[5,6,29]. Our results also provide a benchmark to evaluate ecosystem models (for example, on whether they capture the observed first-order hydroclimatic controls on canopy photosynthetic properties) and highlight the importance of accurately representing the interactions between subsurface water dynamics (including groundwater) and plant functioning. Incorporating these crucial ecohydrological mechanisms can increase confidence in predicting the future of tropical evergreen forests[1,30].

Methods

We studied the hydroclimatic controls on the seasonal variation of photosynthetic properties (as detected by the MODIS EVI and GOME-2 SIF records) of pan-tropical evergreen forests (Amazonia, Africa and Insular SE Asia). We calculated the wet- and dry-season difference in EVI and SIF (denoted as $\Delta EVI_{(wet-dry)}$ and $\Delta SIF_{(wet-dry)}$) for all years of record at the grid level (EVI: 2002–2012; SIF: 2007–2012). For years with no dry season, $\Delta EVI_{(wet-dry)}$ and $\Delta SIF_{(wet-dry)}$ for that specific year were set to zero. We employed the t-test to determine the statistical significance of $\Delta EVI_{(wet-dry)}$ and $\Delta SIF_{(wet-dry)}$ patterns for each grid cell, with the null hypothesis that $\Delta EVI_{(wet-dry)}$ (or $\Delta SIF_{(wet-dry)}$) is equal to zero (paired t-test, $n=11$ years per grid for EVI, and $n=6$ for SIF). EVI is from the 16-day, 0.05 degree MODIS MOD13C1 (Collection 5) product, and only the data flagged as 'good-quality' were used in the analysis. The gaps were filled with a climatology calculated from only 'good-quality' data for any specific grid cell. Thus we claim that our results have more fidelity to address photosynthetic dynamics at seasonal scale than inter-annual scale. Possible artefact of sun-sensor geometry in the MODIS EVI data and its impacts on our results have been addressed in the Supplementary Information. The SIF data used are retrieved near the $\lambda=740$ nm far-red peak in chlorophyll fluorescence emission from the GOME-2 instrument onboard Eumetsat's MetOp-A satellite. The SIF algorithm[13] disentangles three spectral components near the peak of the far-red chlorophyll fluorescence emission feature: atmospheric absorption (due to water vapour), surface reflectance, and fluorescence radiance. The SIF data has been cloud filtered (see Supplementary Information). All of the data sets have been aggregated to a consistent monthly temporal fidelity and 0.5 degree resolution. These data were used to generate Fig. 1d–i and Fig. 2a,b. The spatial patterns of Fig. 1d–i have been smoothed using a 1.5 degree (3×3) square smoothing window.

The wet and dry seasons are distinguished using monthly precipitation and PET. The precipitation data are from the three-hourly, 0.25 degree TRMM Multi-satellite Precipitation Analysis (TMPA) 3B42v6 product, which is adjusted at monthly scale to match gauge data. PET was calculated using the Penman–Monteith equation forced by various climate records and remote sensing data at 0.5 degree resolution from 2002 to 2012. We also calculated PET using a revised Priestley–Taylor approach (see Supplementary Information) with the same forcing records, and found that the two PET algorithms have less than 5% difference in the mean annual range of PET, and thus using either of them does not affect our conclusions.

The threshold value in the mean annual precipitation was optimized such that the negative and positive $\Delta EVI_{(wet-dry)}$ (or $\Delta SIF_{(wet-dry)}$) could be optimally separated based on a single MAP threshold. In particular, we searched for the MAP value to maximize the product of the percentage of negative $\Delta EVI_{(wet-dry)}$ (or $\Delta SIF_{(wet-dry)}$) above this MAP threshold and the percentage of positive $\Delta EVI_{(wet-dry)}$ (or $\Delta SIF_{(wet-dry)}$) below the same MAP threshold. We find that the optimized MAP threshold is 2,025 mm yr^{-1} (95% percentile within [2,002–2,044] mm yr^{-1}) for $\Delta EVI_{(wet-dry)}$, and 2,020 mm yr^{-1} (95% percentile within [2,004–2,043] mm yr^{-1}) for $\Delta SIF_{(wet-dry)}$, which we defined as approximately 2,000 mm yr^{-1}.

The 'dry-season water deficit' is calculated as the cumulative difference between precipitation and PET during the dry season. To identify the subsurface water storage change, we used the ensemble of monthly GRACE terrestrial water storage anomaly data from the three data products[20]. GRACE data was processed using a 300 km-radius Gaussian filter and provided at 1 degree resolution. The coarse spatial resolution of the GRACE data, relative to the other data records used in this study, could have induced errors in our analysis and may explain some of the scatter in the results. We used PET and precipitation data from 2002–2012 to calculate dry-season total water supply deficit for each year, and also calculated the release from water storage from the GRACE data for each dry season. All the data have been aggregated to 1 degree resolution to be consistent with the GRACE data to generate Fig. 3.

Received 21 October 2014; accepted 2 February 2015; published online 9 March 2015

References

1. Huntingford, C. *et al.* Simulated resilience of tropical rainforests to CO_2-induced climate change. *Nature Geosci.* **6,** 268–273 (2013).
2. Restrepo-Coupe, N. *et al.* What drives the seasonality of photosynthesis across the Amazon basin? A cross-site analysis of eddy flux tower measurements from the Brasil flux network. *Agric. For. Meteorol.* **182–183,** 128–144 (2013).
3. Saleska, S., da Rocha, H., Kruijt, B. & Nobre, A. in *Amazonia and Global Change* (eds Keller, M., Bustamante, M., Gash, J. & Silva Dias, P.) 389–408 (American Geophysical Union, 2009).
4. Pan, Y. *et al.* A large and persistent carbon sink in the world's forests. *Science* **333,** 988–993 (2011).
5. Malhi, Y. *et al.* Climate change, deforestation, and the fate of the Amazon. *Science* **319,** 169–172 (2008).
6. Davidson, E. A. *et al.* The Amazon basin in transition. *Nature* **481,** 321–328 (2012).
7. Huete, A. R. *et al.* Multiple site tower flux and remote sensing comparisons of tropical forest dynamics in Monsoon Asia. *Agric. For. Meteorol.* **148,** 748–760 (2008).

8. Huete, A. R. *et al.* Amazon rainforests green-up with sunlight in dry season. *Geophys. Res. Lett.* **33,** L06405 (2006).
9. Da Rocha, H. R. *et al.* Patterns of water and heat flux across a biome gradient from tropical forest to savanna in Brazil. *J. Geophys. Res.* **114,** G00B12 (2009).
10. Guan, K. *et al.* Seasonal coupling of canopy structure and function in African tropical forests and its environmental controls. *Ecosphere* **4,** 1–21 (2013).
11. Huete, A. *et al.* Overview of the radiometric and biophysical performance of the MODIS vegetation indices. *Remote Sens. Environ.* **83,** 195–213 (2002).
12. Van der Tol, C., Berry, J. A., Campbell, P. K. E. & Rascher, U. Models of fluorescence and photosynthesis for interpreting measurements of solar-induced chlorophyll fluorescence. *J. Geophys. Res. Biogeosci.* **119,** 2312–2327 (2014).
13. Joiner, J. *et al.* Global monitoring of terrestrial chlorophyll fluorescence from moderate spectral resolution near-infrared satellite measurements: Methodology, simulations, and application to GOME-2. *Atmos. Meas. Tech.* **6,** 2803–2823 (2013).
14. Bradley, A. V. *et al.* Relationships between phenology, radiation and precipitation in the Amazon region. *Glob. Change Biol.* **17,** 2245–2260 (2011).
15. Saleska, S. R. *et al.* Carbon in Amazon forests: Unexpected seasonal fluxes and disturbance-induced losses. *Science* **302,** 1554–1557 (2003).
16. Myneni, R. B. *et al.* Large seasonal swings in leaf area of Amazon rainforests. *Proc. Natl Acad. Sci. USA* **104,** 4820–4823 (2007).
17. Hilker, T. *et al.* Vegetation dynamics and rainfall sensitivity of the Amazon. *Proc. Natl Acad. Sci. USA* **111,** 16041–16046 (2014).
18. Morton, D. C. *et al.* Amazon forests maintain consistent canopy structure and greenness during the dry season. *Nature* **506,** 221–224 (2014).
19. Pokhrel, Y. N. *et al.* The role of groundwater in the Amazon water cycle: 3. Influence on terrestrial water storage and comparison with GRACE. *J. Geophys. Res. Atmos.* **118,** 3233–3244 (2013).
20. Swenson, S. & Wahr, J. Post-processing removal of correlated errors in GRACE data. *Geophys. Res. Lett.* **33,** L08402 (2006).
21. Pan, M. *et al.* Multisource estimation of long-term terrestrial water budget for major global river basins. *J. Clim.* **25,** 3191–3206 (2012).
22. Nepstad, D. *et al.* The role of deep roots in the hydrological and carbon cycles of Amazonian forests and pastures. *Nature* **3,** 666–669 (1994).
23. Nepstad, D. *et al.* Amazon drought and its implications for forest flammability and tree growth: A basin-wide analysis. *Glob. Change Biol.* **10,** 704–717 (2004).
24. Enquist, B. J. & Enquist, C. A. F. Long-term change within a Neotropical forest: Assessing differential functional and floristic responses to disturbance and drought. *Glob. Change Biol.* **17,** 1408–1424 (2011).
25. Murphy, P. & Lugo, A. Ecology of tropical dry forest. *Annu. Rev. Ecol. Syst.* **17,** 67–88 (1986).
26. Zhou, L. *et al.* Widespread decline of Congo rainforest greenness in the past decade. *Nature* **509,** 86–90 (2014).
27. Phillips, O. L. *et al.* Drought sensitivity of the Amazon rainforest. *Science* **323,** 1344–1347 (2009).
28. Brando, P. M. *et al.* Drought effects on litterfall, wood production and belowground carbon cycling in an Amazon forest: Results of a throughfall reduction experiment. *Phil. Trans. R. Soc. B* **363,** 1839–1848 (2008).
29. Malhi, Y. *et al.* African rainforests: Past, present and future African rainforests: Past, present and future. *Phil. Trans. R. Soc. B* **368,** 20120312 (2013).
30. Cox, P. M., Betts, R. A., Jones, C. D., Spall, S. A. & Totterdell, I. J. Acceleration of global warming due to carbon-cycle feedbacks in a coupled climate model. *Nature* **408,** 184–187 (2000).

Acknowledgements

K.G. and E.F.W. acknowledge financial support from the NASA Earth and Space Science Fellowship (NESSF). J.S.K.'s contribution is supported under the NASA Terra-Aqua Science program (NNX11AD46G). S.R.S. and J.W. acknowledge support by NASA Terra-Aqua Science program (NNX11AH24G) and by DOE Terrestrial Ecosystem Science (DE-SC0008383). We also acknowledge all the data providers for sharing the scientific data.

Author contributions

K.G., M.P. and H.L. conceived the idea; K.G. conducted the analyses; J.W., M.L., S.R.S., J.J. and A.I.L. provided the data; all authors contributed to the writing and revisions.

Additional information

Supplementary information is available in the online version of the paper. Reprints and permissions information is available online at www.nature.com/reprints. Correspondence and requests for materials should be addressed to K.G.

Competing financial interests

The authors declare no competing financial interests.